Sensor-based identification of tool wear in turning

Citation for the original published paper (version of record):
Salame, C., Rapold, R., Tasdelen, B. et al (2024). Sensor-based identification of tool wear in turning. Procedia CIRP, 121: 228-233. http://dx.doi.org/10.1016/j.procir.2023.09.252

Available online at www.sciencedirect.com

ScienceDirect

Procedia CIRP 121 (2024) 228–233

www.elsevier.com/locate/procedia

11th CIRP Global Web Conference (CIRPe 2023)

Sensor-based identification of tool wear in turning

Charlie Salame[a,*], Rico Rapold[a], Bülent Tasdelen[b], Amir Malakizadi[a]

[a]Department of Industrial and Materials Science, Chalmers University of Technology, Gothenburg, Sweden
[b]Kistler Group, Winterthur, Switzerland

* Corresponding author. *E-mail address:* salamec@chalmers.se

Abstract

The online monitoring of tool wear using signal processing during machining has emerged as a prominent technological means in the advancement towards Industry 4.0. In this investigation, the potential of identifying worn cutting tools is assessed using a microphone, 3-axis accelerometer, and 3-axis dynamometer. A comparison of the signals from a sharp versus worn tool shows a potential to identify the wear state of the tool, provided that the suitable signal processing technique and feature selection are employed. The investigation suggests that the careful selection of the sensor's position has a prominent role in the success of the wear identification.

Keywords: machining, monitoring, wear, sensor

1. Introduction

The global shift towards Industry 4.0 has encouraged the integration and broad utilisation of sensors and data analysis within machining processes [1] . Different sensor systems, often coupled with artificial intelligence-supported analysis, have shown great potential in providing time-sensitive information that can maximise the productivity and product quality in manned and unmanned manufacturing systems [2]. To obtain the desired workpiece quality and conform to the tight dimensional tolerances required by the manufacturing industry, it is essential to maintain the integrity of the cutting tool [3]. While some tool wear types such as flank and crater wear are progressive, others such as chipping and notch wear are stochastic, making them difficult to simulate and anticipate [4]. For this reason, modeling attempts generally fail to predict the useful tool life when the mode of failure falls in the stochastic regime. In addition, the simulation of tool wear relies on various simplifications and an abundance of model inputs that increase their complexity and decrease their accuracy [1].

It therefore becomes imperative to integrate real-time tool wear monitoring systems that can provide instantaneous feedback about the tool wear condition, by monitoring the progressive tool wear mechanisms while also signaling the potential occurrence of stochastic wear failure [5]. The implementation of these online monitoring systems allows the manufacturing industry to switch from the conservative time-based tool replacement that is prevalent in industrial systems to a condition-based tool replacement. This would allow the maximisation of the tool's utilisation and thus reduce premature tool changes [6]. Subsequently, productivity would rise given that on average, 20% of cutting machine downtime can be attributed to tool change routines [1,2].

Previous research in the field investigated various methods for tool wear monitoring, which can be predominantly classified into direct and indirect methods [5]. Direct methods such as machine vision and electrical resistance offer the advantage of directly capturing the geometrical changes arising in the wear region of the tool [5,7]. However, the continuous engagement between the cutting tool and workpiece, as well as the flow of chips and coolant in the cutting zone, make direct measurement extremely difficult to implement [8]. This has driven researchers to focus on the development of indirect methods to monitor tool wear, by correlating selected sensors

10.1016/j.procir.2023.09.252

and their specific features to tool wear conditions. Among these, researchers have investigated the use of cutting forces [9], acoustic emissions [10], vibrations [11] and sound pressure [12] among others, all of which provide a greater practicality than the direct methods. Sensor systems used in wear monitoring have been reviewed extensively in literature [1,2,13].

This research investigates the potential for the identification of a worn tool during turning based on indirect monitoring using a 3-axis dynamometer, 3-axis accelerometer, and a microphone. Dry turning of a case-hardening steel is conducted using tools under different wear conditions, including moderate and higher flank wear. A comparative analysis of the obtained signals is then conducted using the Hilbert-Huang (HHT) and wavelet (WT) transformations to investigate the potential of identifying the worn tool using these algorithms. This research acts as an initial assessment of the potential of these methods within the context of tool wear monitoring using accelerometer and microphone. These would present more accessible and cost-effective solutions for industrial applications.

2. Theoretical foundations of the transformations

Traditional data analysis methods such as Fourier transforms are in general based on the assumption that the acquired signal is linear and stationary. Therefore, there is little physical sense to process the highly non-linear and dynamic signals acquired from metal cutting using these transforms [14]. In addition, Fourier transforms employ a convolution integral over the entire data span that does not allow to obtain any local properties of the signal, leading to a loss of transient properties such as decaying frequency components that may identify the onset of tool wear [14]. In contrast, time-frequency analysis methods such as Hilbert-Huang and wavelet transforms overcome these limitations and are able to simultaneously generate the frequency and time data by mapping the acquired one-dimensional signals to the two-dimensional time-frequency plane [14,15].

2.1. Discrete Wavelet Transform

The use of Discrete Wavelet Transform (DWT) in signal processing indicates decomposing the time-varying signal into its component elements with the use of basic functions known as wavelet scale functions [15]. The implementation of the DWT generates a decomposition where the signal is repeatedly passed through high-pass and low-pass filters to yield the detail and scaling functions, respectively. Upon being passed through a high- or low-pass filter, the signal x is convoluted with the filter's impulse response g to yield the discrete function y[n],

$$y[n] = \sqrt{2}(x * g)[n] = \sqrt{2}\sum_{k=-\infty}^{\infty} x[k]g[n-k] \quad (1)$$

At a specific decomposition level in the DWT, the high-pass and low-pass filter that the wavelet functions are passed through should be quadrature mirror filters of each other to ensure the splitting of the input signal into 2 bands. Following each filter convolution, the resulting function is subsampled by a factor of 2 due to half the frequencies of the signal being discarded, thus allowing to discard half of the samples according to the Nyquist criterion. Therefore,

$$y[n] = \sqrt{2}(x * g)[n] \downarrow 2 \quad (2)$$

The output of the subsampled convolution with the high-pass filter then yields the wavelet function of that level, while the low-pass filter yields the scaling function, which are further decomposed in the subsequent decomposition level.

2.2. Hilbert-Huang transform

Similar to the Discrete Wavelet Transform, the Hilbert-Huang Transform (HHT) maps the acquired one-dimensional signal to the time-frequency plane. The HHT operates in a two-step sequence: first, it employs Empirical Mode Decomposition (EMD) to decompose a signal into its intrinsic mode functions (IMF) and second, it applies the Hilbert spectral analysis (HSA) to the obtained IMFs in order to calculate their instantaneous frequency and energy data [14].

The Empirical Mode Decomposition decomposes in the temporal space instead of the corresponding frequency space. The decomposition reveals the signal's IMFs, which are the different oscillatory modes that compose the original signal. The obtained signal then undergoes a sifting process to eliminate background waves and increase the symmetry of the wave profiles. This process is repeated until the sift residual between two successive iterations exceeds a pre-defined value (0.05 in this work) [16]. Once the original signal is decomposed into its mono-component IMFs, the Hilbert transform is then applied to each of the intrinsic functions as follows,

$$y(t) = \frac{p}{\pi}\int_{-\infty}^{\infty} \frac{x(\tau)}{t-\tau} d\tau \quad (3)$$

In Eq. 3, p is the Cauchy principal value of the transform. Then, the Hilbert transform of a signal is its convolution with $1/t$. The analytic signal $z(t)$ is then obtained by coupling the signal $x(t)$ with its Hilbert transform $y(t)$ such that,

$$z(t) = x(t) + iy(t) = a(t)e^{i\varphi(t)} \quad (4)$$

with $a(t) = \sqrt{x^2(t) + y^2(t)}$ (5)

and $\varphi(t) = \tan^{-1}\left(\frac{y(t)}{x(t)}\right)$. (6)

In Eq. 4, 5, and 6, $a(t)$ and $\varphi(t)$ are respectively the amplitude and instantaneous phase of the analytic signal $z(t)$. The instantaneous frequency $w(t)$ can then be obtained by,

$$w(t) = \frac{d\varphi(t)}{dt} \quad (7)$$

Advantages of the HHT method include its preservation of the length of the original signal given the transient phenomena occurring in different time intervals along the signal, as well as its preservation of the signal's varying frequency due to its use of EMD.

3. Experimental setup and measurement system

3.1. Experimental procedure

The longitudinal cutting of a case hardening steel with a carbon content of 0.2 wt% (pearlitic-ferritic microstructure - 170 HBW) was conducted on an EMCO TURN 365. The chemical composition of the material grade cannot be revealed due to proprietary restrictions. The CVD-coated carbide inserts (DCMT11T304-M3 TP2501 Seco Tools grade) were mounted on a DDJCR2525-X11-JETI tool holder, such that the nominal rake angle was 0° and the clearance angle was 7°. The cutting speed was kept constant at 150 m/min and the depth of cut at 1 mm for all cutting conditions. The feed was varied in three levels: 0.20, 0.25 and 0.30 mm/rev. All machining tests were performed for a constant spiral cutting length of 30 m. Fig. 1 shows the experimental setup used for the machining tests.

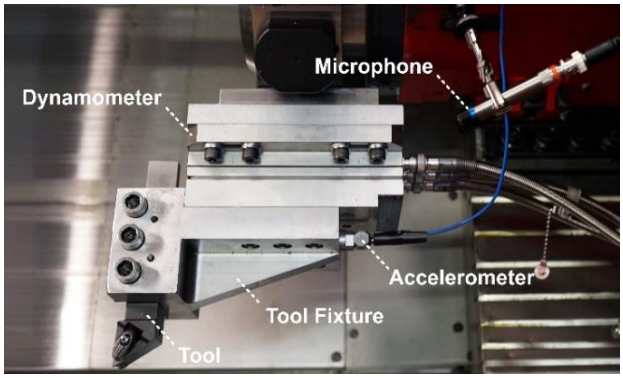

Fig. 1. Experimental setup used for dry longitudinal turning (with the accelerometer placed in position 01)

The cutting tests were performed for different cutting conditions using inserts with different wear conditions, as detailed in Table 1. For statistical validity, cutting tests A1, A2, B1, B2, C1 and C2 were repeated 9 times while tests A3 and A4 were repeated 3 times.

Table 1. Cutting and tool wear conditions.

No.	Feed [mm/rev]	Tool Condition	Accelerometer Position
A1	0.20	New	01
A2	0.20	Flank wear [VB = 220 ± 20μm]	01
A3	0.20	Flank wear [VB = 340 ± 20μm]	01
A4	0.20	Flank wear [VB = 340 ± 20μm]	02
B1	0.25	New	01
B2	0.25	Flank wear [VB = 220 ± 20μm]	01
C1	0.30	New	01
C2	0.30	Flank wear [VB = 220 ± 20μm]	01

3.2. Sensors and data acquisition system

To measure the cutting forces during the longitudinal turning experiments, the CNC-lathe was equipped with a three-component dynamometer (Kistler 9257A), as shown in the schematic representation in Fig. 2. The tri-axial dynamometer was connected to a Kistler Type 5001 charge amplifier having 3 channel inputs with gain settings and outputting 3 voltage signals, one for each of the force components, i.e., cutting force F_c, feed force F_f and passive force F_p. After amplification, the signals for the force components were fed to the Data Acquisition (DAQ) system, which is a National Instruments PXI-4462 module mounted onto a PXI-1033 chassis.

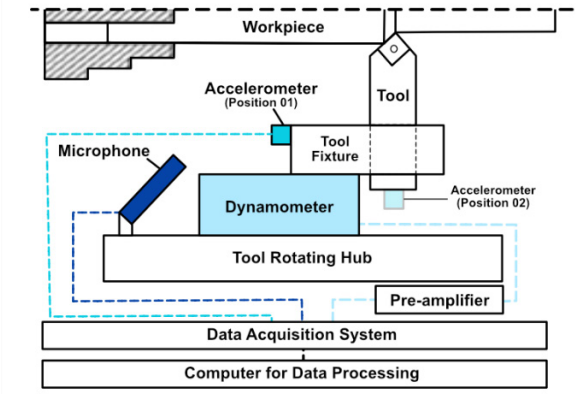

Fig. 2. Schematic representation of sensors and data acquisition system.

The accelerometer used to measure the acceleration during the cutting process was of type 8766A050 from Kistler Group. It measured the acceleration in 3 directions: a_x, a_y and a_z in the cutting, feed and passive directions respectively. The accelerometer possesses a sensitivity of 100mV/g and exhibits a self-resonance effect up to 10% in the measuring range up to 8 kHz. Therefore, a low-pass filter of elliptic type was placed at 8 kHz in order to reduce the noise level in the measurements. Lastly, the acquisition rate of the sensor was set to 50kHz to satisfy the Nyquist criteria and avoid aliasing.

Given the exposure to cutting fluids and chips within industrial machines, the placement of the accelerometer is not subject to a lot of flexibility. The position of the accelerometer is further constrained by its measuring range (±50g), where it has to be close enough to the cutting zone to detect the subtle variations in the signals but also not exceed the accelerometer's allowed measuring range and be exposed to the exiting chips if placed too close. For those reasons, this research conducted a preliminary investigation into the sensitivity of the accelerometer measurements to its position. The accelerometer was placed in 2 different positions, as shown in Fig. 2: on the tool fixture (Position 01) and directly on the back side of the tool (Position 02).

Lastly, a 146AE GRAS microphone was used to measure the sound pressure S_M during the cutting process with a sensitivity of 50mV/Pa. The recommended range for measurements using this particular microphone is 0-20kHz; therefore, the low-pass filter was set at 20kHz and the sampling rate to 50kHz for anti-aliasing purposes. The signals from both the accelerometer and the microphone were directly fed into the DAQ, as shown in Fig. 2. Then, the DAQ sent the data to the connected computer for processing.

3.3. Signal processing

During each cut, the DAQ collected 7 signals in total: F_c, F_f, F_p, a_x, a_y, a_z and S_M. No signal shifting was required since the data collected by the DAQ was already synced to the same time scale. Signal segmentation was then carried out on each of the acquired signals in order to extract a portion corresponding to 6 seconds of the cutting phase. The signal sections where the tool was not engaged with the workpiece were discarded.

For the cutting force measurements, the acquired voltage signal for each direction was multiplied by the corresponding

calibration constant to yield the equivalent force in Newtons. Then, the signal's mean value was extracted, and the resulting cutting force values were compared for a new and worn edge.

The Discrete Wavelet transform was applied to the signals acquired from the accelerometer (a_x , a_y and a_z) and microphone (M_{SP}). Each of the four signals was decomposed to the 7th level and the wavelet function obtained for each level was then treated as a separate signal from which relevant statistical features could be extracted. This research employed the root-mean-square (RMS) value of the obtained coefficients for each level to compare between the different tool wear states.

The success rate in identifying the worn tool was determined as follows. Each signal was decomposed into seven wavelets, for which the RMS value of each was obtained. Based on the analysis of the data at a specific wavelet level, it was noted that the RMS value for a worn insert was generally smaller than the RMS value of a sharp tool for a given cutting condition. This pattern, of course, depends on the wavelet level analysed and may not be generalized to all cases; however, in the signals analysed in this research, a decrease in RMS value for a worn tool seemed to be the more frequent occurrence. Based on this observation, the range of RMS values for a new tool was determined from multiple repetitions for each cutting condition. Then, the success rate for identifying the worn tool was determined as the ratio of the discriminated worn cases (where the RMS-value fell below the new tool's RMS range) divided by the number of repetitions for that cutting condition.

For the lower level of wear [VB=220±20μm], 9 cuts with a sharp edge were compared against 9 cuts with a worn tool. Since the tool wear progression is considerably faster at the higher level of wear [VB=340±20μm], less cuts could be completed before the tool reached failure. Thus, 3 cuts were compared using a worn tool versus 3 cuts with a new tool.

In the case of the Hilbert-Huang transform, the 4 acquired signals (a_x, a_y, a_z and M_{SP}) were decomposed using EMD after which the Hilbert spectral analysis was applied. The algorithm then considered the first 4 IMFs of each signal and extracted the relevant features for tool wear identification. Since the first IMF generally carries the high-frequency components of the signal, it can be rejected since it is most likely distorted by noise [14]. Therefore, the HHT analysis in this research focuses on the 2nd, 3rd and 4th IMFs in order to distinguish between a new and worn tool. In this investigation, the extracted feature for tool wear identification was the average energy associated with each IMF function. Similar to the DWT analysis, the range of the extracted feature was determined for a new tool, after which the energy values for the worn tool were compared against the obtained range.

4. Results and Discussions

4.1. Identification of wear using cutting forces

A comparison of the average cutting forces obtained for each of the cutting conditions is presented in Table 2. When comparing the mean values of the cutting forces for the same cutting condition, an increase in all 3 force components is evident for the case of the worn tool, especially for the feed and passive forces. For instance, for a cutting feed of 0.25mm/rev, a flank wear of 220 ± 20μm induces an increase of 4%, 68% and 155% in F_c, F_f and F_p respectively when compared to a sharp cutting edge. The increase becomes more prominent as the wear progresses, as seen when comparing cutting conditions A3 to A2. When the flank wear increases from 220 ± 20μm to 340 ± 20μm, the cutting, feed and passive forces increase by 15%, 80% and 82% respectively for a feed of 0.2mm/rev. Despite their success in identifying tool wear, dynamometers can be unattractive for industrial applications due to their high cost, low adaptability to different machinery and their fastening which can require structural changes to the machine [17].

Table 2. Cutting force measurements for the different cutting conditions.

No.	Tool Condition	F_c [N]	F_f [N]	F_p [N]
A1	New	396±22	172±17	79±5
A2	Flank wear [VB=220 ± 20μm]	415±9	229±2	160±2
A3	Flank wear [VB=340 ± 20μm]	478±17	412±12	290±12
A4	Flank wear [VB=340 ± 20μm]	465±19	393±23	285±10
B1	New	477±12	178±3	92±3
B2	Flank wear [VB=220 ± 20μm]	495±4	299±3	235±7
C1	New	547±13	186±3	105±2
C2	Flank wear [VB=220 ± 20μm]	567±4	271±6	217±6

4.2. Identification of wear using sound pressure

The Discrete Wavelet and Hilbert-Huang analysis of the microphone's signals during machining showed varied success in identifying tool wear, with the HHT method being overall the more successful of the two. For instance, Fig. 3 shows the HHT analysis comparisons between cuts B1 (sharp edge) and B2 (VB=220 ± 20μm). As shown, the HHT method manages to identify the worn tool using all of the 4 IMFs with the success rates for each IMF reported in Table 3.

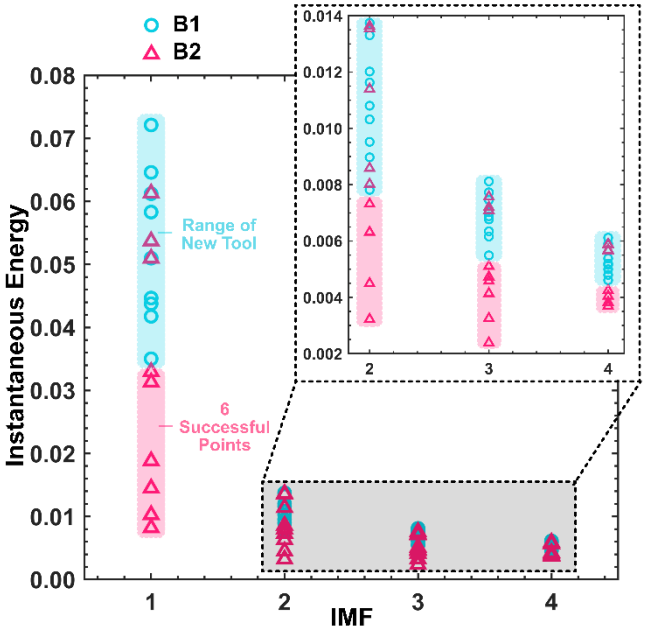

Fig. 3. HHT analysis of microphone signals for cutting conditions B1 and B2.

In contrast, the DWT analysis fails to identify the worn tool in most cases for this cutting condition as observed in Fig. 4.

When applied to the different cutting conditions, Table 3 presents the success rate (in percentage) of each level/IMF in differentiating worn from unworn tools. As evident, the DWT method fails to successfully identify the worn tool in the majority of the cases. On the other hand, the HHT method performed significantly better, having a success rate of up to 78% in identifying the tool with VB=$220 \pm 20\mu$m using the 2nd and 3rd IMF functions.

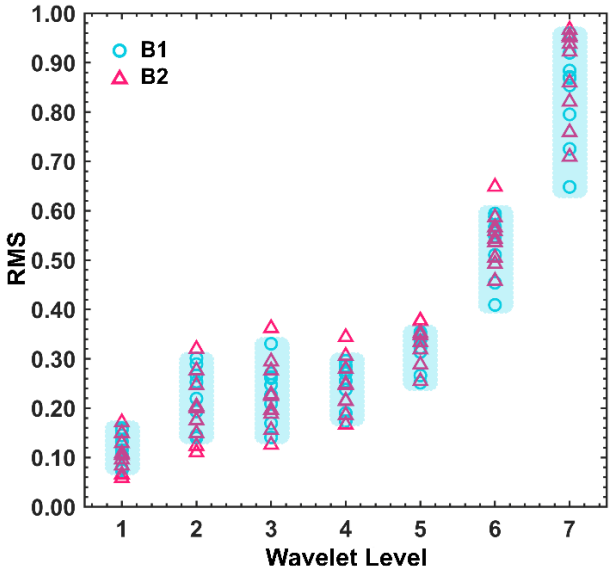

Fig. 4. DWT analysis of microphone signals for cutting conditions B1 and B2.

Table 3. Success rates in predicting tool wear for DWT and HHT analysis of the microphone signals

Method	Level	Tool and Cutting Condition			
		A2	A3	B2	C2
DWT	1	0%	0%	22%	11%
	2	0%	0%	22%	67%
	3	0%	0%	11%	67%
	4	0%	0%	11%	67%
	5	0%	0%	0%	22%
	6	0%	0%	0%	22%
	7	0%	0%	0%	22%
IMF	1	67%	67%	67%	67%
	2	33%	67%	44%	78%
	3	78%	67%	67%	67%
	4	56%	67%	44%	44%

4.3. Identification of wear using acceleration

Similar to the sound pressure, the accelerometer signals showed varied levels of success in identifying the worn tool, depending on the direction of the acceleration. Using the DWT method, the highest success rates were obtained using the passive direction of acceleration (a_z), as presented in Table 4. In addition, the acceleration in the cutting direction (a_x) yielded a maximum success rate of 56% using both the 2nd and 3rd wavelet levels for cutting conditions B2 and C2. The acceleration in the feed direction (a_y) yielded a maximum success rate of 44% using the 4th wavelet level for cutting condition C2.

Table 4. Success percentage of tool wear identification using DWT of acceleration signal a_z

Signal	Level	Tool and Cutting Condition				
		A2	A3	B2	C2	A4
a_z	1	22%	33%	11%	22%	0%
	2	22%	33%	11%	33%	0%
	3	44%	100%	22%	56%	0%
	4	44%	0%	56%	67%	0%
	5	44%	100%	56%	56%	33%
	6	11%	33%	11%	22%	33%
	7	0%	0%	0%	22%	0%

In contrast, the Hilbert-Huang transform showed more promise by successfully identifying the worn tool as detailed in Table 5. In general, the 2nd and 3rd IMF functions in the feed and passive directions exhibit an improved success rate in identifying the worn tool.

Given that this work was an initial assessment of these methods' potential, future work can improve the success rate by extracting and correlating more features from the IMF functions and DWT wavelets. Different decomposition methods may be investigated in order to enhance the HHT method's rigor in identifying worn tools. In addition, improvements can be made by implementing a fusion of sensor inputs and integrating AI-based decision-makers for different tool-workpiece combinations and cooling environments.

Table 5. Success percentage of tool wear identification using HHT of the acceleration signals.

Signal	IMF	Tool and Cutting Condition				
		A2	A3	B2	C2	A4
a_x	1	56%	33%	44%	67%	0%
	2	11%	0%	0%	0%	100%
	3	0%	0%	11%	0%	67%
	4	0%	100%	0%	0%	100%
a_y	1	22%	67%	89%	33%	0%
	2	89%	100%	78%	56%	0%
	3	33%	100%	44%	11%	0%
	4	11%	0%	0%	0%	67%
a_z	1	44%	100%	67%	44%	0%
	2	44%	100%	56%	44%	67%
	3	44%	100%	67%	33%	0%
	4	11%	0%	11%	22%	67%

4.4. Sensitivity of the accelerometer data to its position

By varying the accelerometer position from position 01 to position 02, as shown in Fig. 2 and Table 5, the sensitivity of the wear identification to the accelerometer position was assessed. It is evident from the results in Fig. 5 and Table 5 that there is a significant effect of the accelerometer position on the tool wear identification, owing largely to the difference in stiffness of the different components within the machine. Counterintuitively, placing the accelerometer directly on the tool holder as opposed to the tool fixture led to a decrease in the ability of the algorithm to identify the worn tool. Further research is required to investigate the reasons behind this observation. Yet, this perhaps highlights the importance of tailoring the sensor placement in industrial applications to yield the highest success rates of tool wear identification.

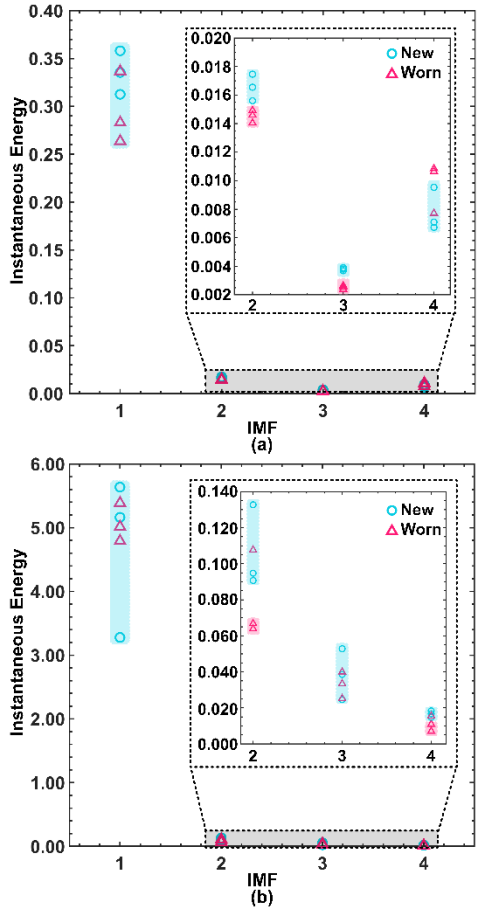

Fig. 5. Comparison of HHT instantaneous energies obtained from accelerometer a_y signal in (a) position 01 and (b) position 02

5. Conclusions

This research investigated the ability of different sensor signals combined with different data analysis techniques to identify flank wear in cutting tools used for longitudinal turning. From an industrial perspective, the microphone seems to be the most attractive sensor combining fairly high success rates with high flexibility in its positioning. While the accelerometer has a higher success rate, it possesses a higher cost and lower flexibility in positioning since it needs to be attached directly to the tool setup. The main findings of this work are:

- The dynamometer successfully identified flank wear with an increase in cutting, feed and passive forces.
- The DWT method based on the RMS value of the wavelet coefficients failed to successfully identify the worn tool using both acceleration and sound signals.
- Using HHT analysis, the sound signal was able to successfully identify the worn tool in up to 78% of the cases of flank wear (VB=220 $\pm$ 20μm) based on the maximum instantaneous energy in the 3rd IMF.
- The acceleration signals analysed using HHT showed good potential in identifying the worn tool, especially utilising the 2nd and 3rd IMF function in the feed direction, which yielded up to 100% success rate.
- The tool wear identification success rates showed considerable sensitivity to the position of the accelerometer, indicating an importance to tailor its positioning in industrial applications.

Acknowledgements

This study was part of the WEAR-FRAME project funded by Vinnova (Sweden´s Innovation Agency) under FFI program (Project No.2020-05179). The supports received from the Chalmers Area of Advance – Production and the Chalmers Centre for Metal Cutting Research (MCR) are acknowledged.

References

[1] Kuntoğlu, M., Salur, E., Gupta, M. K., Sarıkaya, M., and Pimenov, D. Y., 2021, "A State-of-the-Art Review on Sensors and Signal Processing Systems in Mechanical Machining Processes," The International Journal of Advanced Manufacturing Technology, **116**, pp. 2711–2735.
[2] Rehorn, A. G., Jiang, J., and Orban, P. E., 2005, "State-of-the-Art Methods and Results in Tool Condition Monitoring: A Review," The International Journal of Advanced Manufacturing Technology, **26**, pp. 693–710.
[3] Ratava, J., Lohtander, M., and Varis, J., 2017, "Tool Condition Monitoring in Interrupted Cutting with Acceleration Sensors," Robotics and Computer-Integrated Manufacturing, **47**, pp. 70–75.
[4] Wang, P., and Gao, R. X., 2016, "Stochastic Tool Wear Prediction for Sustainable Manufacturing," Procedia CIRP, **48**, pp. 236–241.
[5] Li, N., Chen, Y., Kong, D., and Tan, S., 2017, "Force-Based Tool Condition Monitoring for Turning Process Using v-Support Vector Regression," The International Journal of Advanced Manufacturing Technology, **91**, pp. 351–361.
[6] Caggiano, A., 2018, "Tool Wear Prediction in Ti-6Al-4V Machining through Multiple Sensor Monitoring and PCA Features Pattern Recognition," Sensors, **18**(3), p. 823.
[7] García-Pérez, A., Ziegenbein, A., Schmidt, E., Shamsafar, F., Fernández-Valdivielso, A., Llorente-Rodríguez, R., and Weigold, M., 2023, "CNN-Based in Situ Tool Wear Detection: A Study on Model Training and Data Augmentation in Turning Inserts," Journal of Manufacturing Systems, **68**, pp. 85–98.
[8] Sick, B., 2002, "On-Line and Indirect Tool Wear Monitoring in Turning with Artificial Neural Networks: A Review of More than a Decade of Research," Mechanical systems and signal processing, **16**(4), pp. 487–546.
[9] Kong, D., Chen, Y., Li, N., and Tan, S., 2017, "Tool Wear Monitoring Based on Kernel Principal Component Analysis and V-Support Vector Regression," The International Journal of Advanced Manufacturing Technology, **89**(1), pp. 175–190.
[10] Jemielniak, K., Urbański, T., Kossakowska, J., and Bombiński, S., 2012, "Tool Condition Monitoring Based on Numerous Signal Features," The Int. Journal of Advanced Manufacturing Technology, **59**, pp. 73–81.
[11] Stavropoulos, P., Papacharalampopoulos, A., and Souflas, T., 2020, "Indirect Online Tool Wear Monitoring and Model-Based Identification of Process-Related Signal," Advances in Mechanical Engineering, **12**(5).
[12] Joseph, E. R., Kiong, L. C., Soong, L. W., and Purushothaman, S., 2012, "Emitted Sound Amplitude Analysis Using Hilbert Huang Transformation for Cutting Tool Flank Wear Prediction," *Global Trends in Computing and Communication Systems: 4th International Conference, ObCom 2011, Vellore, TN, India, December 9-11, 2011. Proceedings, Part I*, Springer, pp. 743–752.
[13] Colantonio, L., Equeter, L., Dehombreux, P., and Ducobu, F., 2021, "A Systematic Literature Review of Cutting Tool Wear Monitoring in Turning by Using Artificial Intelligence Techniques," Machines, **9**(12).
[14] Huang, N. E., and Wu, Z., 2008, "A Review on Hilbert-Huang Transform: Method and Its Applications to Geophysical Studies," Reviews of geophysics, **46**(2).
[15] Li, X., 2002, "A Brief Review: Acoustic Emission Method for Tool Wear Monitoring during Turning," International Journal of Machine Tools and Manufacture, **42**(2), pp. 157–165.
[16] Wang, G., Chen, X.-Y., Qiao, F.-L., Wu, Z., and Huang, N. E., 2010, "On Intrinsic Mode Function," Advances in Adaptive Data Analysis, **2**(03).
[17] Pimenov, D. Y., Bustillo, A., Wojciechowski, S., Sharma, V. S., Gupta, M. K., and Kuntoğlu, M., 2022, "Artificial Intelligence Systems for Tool Condition Monitoring in Machining: Analysis and Critical Review," Journal of Intelligent Manufacturing, pp. 1–43.